PERGAMON

International Journal of Heat and Mass Transfer 46 (2003) 481–495

International Journal of HEAT and MASS TRANSFER

www.elsevier.com/locate/ijhmt

Heat transfer and friction behaviors in rectangular channels with varying number of ribbed walls

P.R. Chandra [a,*], C.R. Alexander [a], J.C. Han [b]

[a] Department of Mechanical Engineering, McNeese State University, P.O. Box 91735, Lake Charles, LA, 70609 USA

[b] Department of Mechanical Engineering, Texas A&M University, College Station, TX, 77843 USA

Received 10 April 2001; received in revised form 25 June 2002

Abstract

An experimental study of surface heat transfer and friction characteristics of a fully developed turbulent air flow in a square channel with transverse ribs on one, two, three, and four walls is reported. Tests were performed for Reynolds numbers ranging from 10,000 to 80,000. The pitch-to-rib height ratio, P/e, was kept at 8 and rib-height-to-channel hydraulic diameter ratio, e/D_h was kept at 0.0625. The channel length-to-hydraulic diameter ratio, L/D_h, was 20. The heat transfer coefficient and friction factor results were enhanced with the increase in the number of ribbed walls. The friction roughness function, $R(e^+)$, was almost constant over the entire range of tests performed and was within comparable limits of the previously published data. The heat transfer roughness function, $G(e^+)$, increased with roughness Reynolds number and compared well with previous work in this area. Both correlations could be used to predict the friction factor and heat transfer coefficient in a rectangular channel with varying number of ribbed walls. The results of this investigation could be used in various applications of turbulent internal channel flows involving different number of rib roughened walls.

1. Introduction

Repeated ribs or turbulators have been used as the promoters of turbulence to enhance the heat transfer to the flow of coolants in a channel. These roughness elements break the laminar sub-layer of the flow. The heat transfer is enhanced as well as the pressure drop, an important parameter in the analysis of the overall performance of such flows. Investigations have been conducted to predict the effect of the number of ribbed walls on heat transfer and friction characteristics. In applications such as cooling of gas turbine airfoils, rib turbulators are cast mostly on two opposite sides of the cooling channels, since the heat transfer takes place from the inner walls of the pressure and the suction sides of the blade. However, in some cases, rib turbulators are cast on one side or four sides of the cooling channels. While turbine blade internal cooling has been widely studied in the past, other applications such as electronic equipment, heat exchangers, and nuclear reactors may utilize the results of enhanced internal cooling in channels with one, two, three, or all four rib-roughened walls. The results with four-ribbed wall channel are also used to validate the assumptions made in the past to develop semi-empirical correlations for friction and heat transfer roughness functions.

Several publications have addressed the state-of-the-art review of turbine blade cooling and the analysis of heat transfer and friction characteristics of the channel flow with two opposite ribbed walls. The effects of flow Reynolds number and rib geometry (rib height, rib spacing, rib angle-of-attack, and rib configuration) on heat transfer and pressure drop in the fully developed region of uniformly heated square channels have been investigated [1,2]. Further study of the combined effects

* Corresponding author. Tel.: +1-337-475-5856; fax: +1-337-475-5237.

E-mail address: pchandra@mail.mcneese.edu (P.R. Chandra).

0017-9310/03/$ - see front matter © 2002 Elsevier Science Ltd. All rights reserved.
PII: S0017-9310(02)00297-1

Nomenclature

AR	aspect ratio $= W/H$
A	heat transfer surface area
C	total combined width of the channel walls $= C_r + C_s$
D	channel diameter
e	rib height
e^+	roughness Reynolds number
f	friction factor
$G(e^+)$	heat transfer roughness function
g_c	conversion factor
H	flow channel height
h	heat transfer coefficient
k	thermal conductivity of air
L	channel length
$\dot{m}$	flow mass velocity
$Nu, \overline{Nu}$	Nusselt number $= hD_h/k$, average Nusselt number
P	rib pitch
Pr	Prandtl number of air
Δp	pressure drop across the test section
q	heat generation rate from the heaters
q_{loss}	heat loss rate through insulation
Re	Reynolds number $= \rho D_h V/\mu$
$R(e^+)$	friction roughness function
St	Stanton number $= Nu/[(Re)(Pr)]$
T	temperature
V	average air velocity
W	flow channel width
X	axial distance from the channel inlet

Greek symbols

μ	average dynamic viscosity of air
ρ	average density of air

Subscripts

b	bulk mean
h	hydraulic
r	ribbed wall
rr	four ribbed walls
s	smooth wall
ss	four smooth walls
w	local wall

of rib geometry and channel aspect ratio on the local values of heat transfer and pressure drop was also reported [3–5]. The results show that the angled ribs provide a better heat transfer performance than transverse ribs, and the lower aspect ratio (AR) channels perform better than the higher aspect ratio channels. The heat/mass transfer analogy has been applied to study detailed heat transfer distribution in two-pass and three-pass rectangular channels [6–10]. The square channel with parallel and crossed arrays of cross cut and beveled discrete ribs has been studied [11,12]. Also, the effect of the equally segmented ribs arranged in both aligned and staggered arrays on two opposite walls of a square channel has been reported [13].

The semi-empirical correlations over a wide range of rib geometry for the friction and heat transfer design calculations are derived from the law of the wall similarity for flow over rough surfaces. The similarity law concept was first developed by Nikuradse [14], who applied it successfully to correlate the friction data for fully developed turbulent flow in tubes with sand roughness. Based on the heat-momentum transfer analogy, Dipprey and Sabersky [15] developed the heat transfer similarity law for fully developed turbulent flow in tubes with sand roughness. Webb et al. [16] extended the similarity law for turbulent tube flow with repeated ribs and Han et al. [17] applied the similarity law for turbulent channel flow with two opposite ribbed walls. Han [1,3] presented a detailed analysis of the application of the similarity laws for rectangular channels with two opposite ribbed walls.

An objective of this study is to investigate the effect of number of ribbed walls on the friction factor and heat transfer coefficient in a ribbed channel. In the past, most of the experiments have been done for rectangular channels with two opposite ribbed walls. The present study extends its base to provide experimental data for square channels with one, two, three, and four ribbed walls. Another objective of the present research is to develop friction and heat transfer correlations not only for rectangular channels with two opposite ribbed walls but also for rectangular channels with one, three, or four ribbed walls.

Experiments have been conducted to investigate the heat transfer and friction characteristics of turbulent flow of air in a divided (ten sections) square channel (3.81 cm × 3.81 cm cross-section). The walls of the square channel (AR = 1) are roughened with full transverse ribs. The rib placement on each roughened wall is identical. The flow Reynolds number for this study ranges from 10,000 to 80,000. The channel length-to-hydraulic diameter ratio, L/D_h, is kept at 20; the rib height-to-hydraulic diameter ratio, e/D_h, is kept at 0.0625; and the rib pitch-to-height ratio, P/e, is kept at 8. In all, five cases are studied (Fig. 1). Figs. 2 and 3, respectively, show the schematic of the test rig and cross-

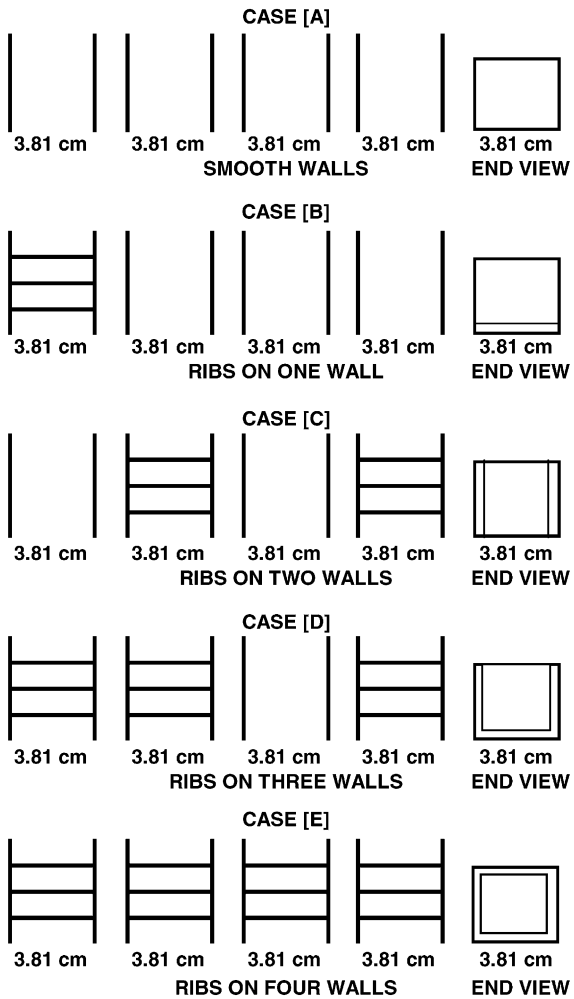

Fig. 1. Rib configurations.

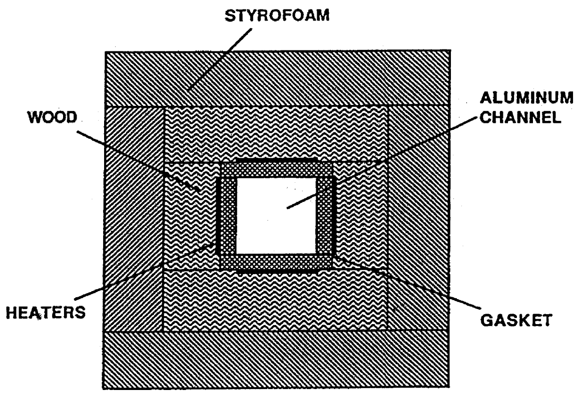

Fig. 3. Cross-section of the test channel.

section of the test channel. A description of the present experimental apparatus could be found in Chandra et al. [18] for a rectangular channel (AR = 0.5) with varying number of ribbed walls.

2. Theory

The semi-empirical correlations developed in the past were based on the assumption that the friction factor and the rib-sided heat transfer coefficients in a channel with two smooth and two ribbed walls can be calculated from geometrically similar channels with four smooth walls and four ribbed walls, Han [1,3]. The values from four-sided smooth and four-sided ribbed walls cases are weighed proportionally to the cross-sectional widths of the smooth and the ribbed walls. There was no experimental verification of this assumption.

The channel pressure drop, Δp, is the weighted average of the four-sided smooth channel pressure drop, Δp_{ss}, and the four-sided ribbed channel pressure drop, Δp_{rr}. These pressure drops are weighted by the total smooth wall cross-sectional width, C_s, and the total ribbed wall cross-sectional width, C_r, Han [3].

Pressure drop in a ribbed channel can be expressed as sum of:

$$\Delta p_r = \Delta p_{ss}(C_s/C) + \Delta p_{rr}(C_r/C) \tag{1}$$

thus from a force balance in a ribbed channel:

$$f_r = f_{ss}(C_s/C) + f_{rr}(C_r/C) \tag{2}$$

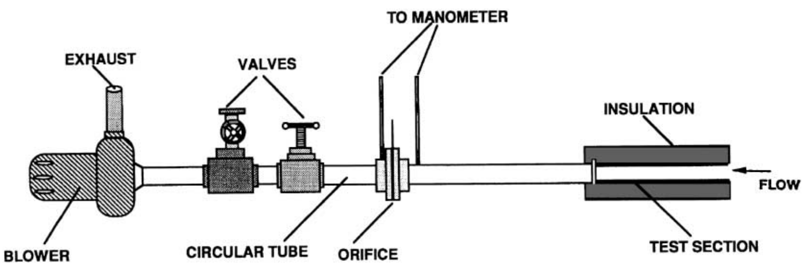

Fig. 2. Schematic of the test rig.

Based on the above theory, three situations with different rib placements are illustrated below:

$$e^+ = (e/D_h)Re(f_{rr}/2)^{1/2} \tag{7}$$

and

$$Z = 2AR/(1 + AR); \quad AR = W/H \tag{8}$$

Example 1: Channel with rib on one side

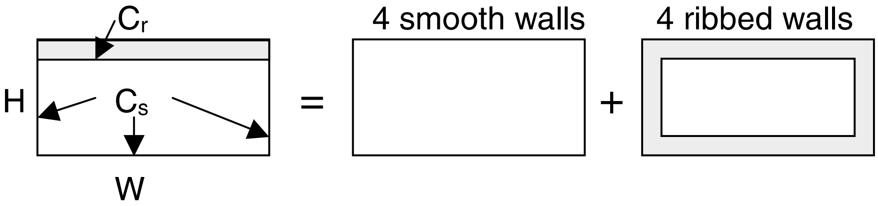

$$f_r = f_{ss}(2H + W)/(2(H + W)) + f_{rr}(W)/(2(H + W)) \tag{3}$$

Example 2: Channel with rib on two sides

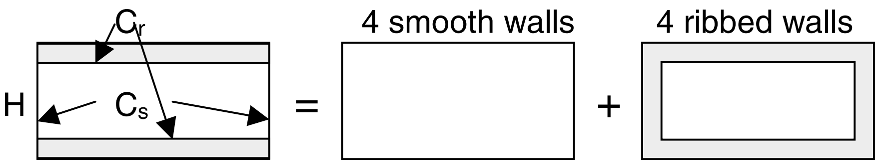

$$f_r = f_{ss}(2H)/(2(H + W)) + f_{rr}(2W)/(2(H + W)) \tag{4}$$

Example 3: Channel with rib on three sides

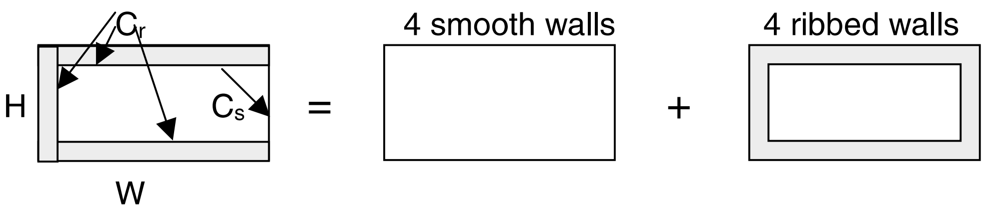

$$f_r = f_{ss}(H)/(2(H + W)) + f_{rr}(H + 2W)/(2(H + W)) \tag{5}$$

This force balance analysis shows the relationship between the friction factor in a one-wall (two-walls or three-walls) ribbed channel and that in a four-walls ribbed channel from Han [1,3]. The friction similarity law for turbulent flow in ribbed rectangular channels was based on flow in a four-walls ribbed channel. The similarity law correlated the four-sided ribbed channel friction factor (f_{rr}) data into a so-called friction roughness function ($R(e^+)$) for rectangular channels with different aspect ratio (AR) with geometrically similar ribs (e/D_h). This can be expressed as Eq. (6), from Han [3].

$$R(e^+) = (f_{rr}/2)^{-1/2} + 2.5\ln((2e/D_h)Z) + 2.5 \tag{6}$$

where

However, most of previous experimental data were obtained for flow in rectangular channels with two opposite ribbed walls. Therefore, Eq. (4) was assumed to get the four-walled rib channel f_{rr} from experimental two-wall rib channel f_r for a given Z or AR(W/H) and a known smooth channel f_{ss} at a given Reynolds number. Then the predicted f_{rr} was used in Eq. (6) for determining friction roughness function $R(e^+)$.

In the present study, the following Eq. (9), which is based on the analysis from Eqs. (3)–(5), can be used to get f_{rr} from experimental f_r as

$$f_{rr} = f_r + (C_s/C_r)(f_r - f_{ss}) \tag{9}$$

where, C_r and C_s depend on one-sided, two-sided, three-sided, or four-sided ribbed walls as shown in Eqs. (3)–(5).

Similarly, the similarity law correlated the four-sided ribbed channel Stanton number (St_{rr}) data into a so-called heat transfer roughness function ($G(e^+)$) for rectangular channel with different aspect ratio (AR) with geometrically similar ribs (e/D_h). This can be expressed as Eq. (10), from Han [3].

$$G(e^+) = ((f_{rr}/2)^{1/2})/St_{rr} + 2.5\ln((2e/D_h)Z) + 2.5 \quad (10)$$

However, most of previous experimental data were obtained for flow in rectangular channel with two opposite ribbed walls. The area-weight friction factor analysis such as Eq. (9) cannot be directly applied for the heat transfer case. Therefore, the relationships between the four-sided ribbed channel St_{rr} and the one-sided, two-sided or three-sided ribbed channel must be determined experimentally. In the present study, the following Eq. (11) has been correlated from the present experimental data

$$St_{rr} = (C_r/C)^{-0.15} St_r \quad (11)$$

where the power "–0.15" was from data fitting, and St_r is from experimental Nu_r data as

$$St_r = Nu_r/(Re\ Pr) \quad (12)$$

From the above mentioned theory, we can correlate all experimental friction (f_r) and heat transfer (St_r) data into $R(e^+)$ and $G(e^+)$ functions, respectively, for various turbulent flows in rectangular channels with different aspect ratios (AR) with varying number of ribbed walls (i.e., one-sided, two-sided, three-sided or four-sided rib walls). Our purpose here is to correlate the limited data into $R(e^+)$ and $G(e^+)$ functions. Once we have obtained the function of $R(e^+)$ and $G(e^+)$, then the designers or users can use these $R(e^+)$ and $G(e^+)$ to predict f_{rr} from Eq. (6) (then f_r from Eq. (9)) and St_{rr} from Eq. (10) (then St_r from Eq. (11)) for a given AR channel with one-sided, two-sided, three-sided or four-sided rib walls at a given e/D_h value and flow Reynolds number.

3. Data reduction

The friction factor in a ribbed channel can be defined in terms of the pressure drop and the air mass velocity and can be calculated for a fully developed flow from

$$f_r = \Delta p_r/[4(L/D_h)(\dot{m}^2/2\rho g_c)] \quad (13)$$

The friction factor is normalized by the friction factor for fully developed turbulent flow in smooth circular tube ($10^4 < Re < 10^6$) proposed by Blasius [19] as:

$$f_r/f_{ss} = f_r/[0.046 Re^{-0.2}] \quad (14)$$

The local (regionally averaged) heat transfer coefficient is calculated from the local net heat transfer rate per unit area to the cooling air, the local wall temperature, and the local bulk mean air temperature as:

The local net heat transfer rate for the smooth and the ribbed walls is the power supplied to the respective heaters minus the heat loss from the test duct to the atmosphere

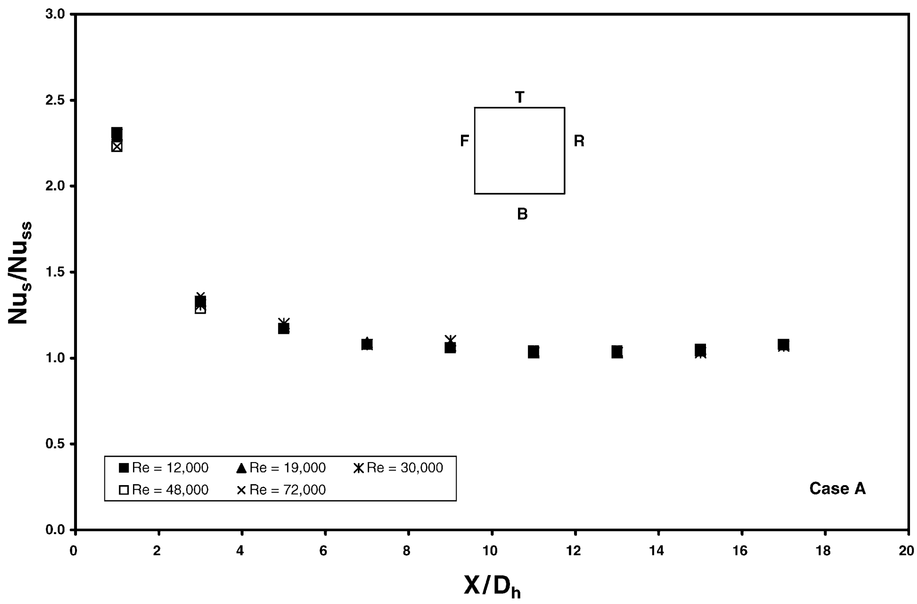

Fig. 4. Axial heat transfer distributions for smooth channel.

$$h_r = (q - q_{\text{loss}})/[A_r(T_w - T_b)] \quad \text{or}$$
$$h_s = (q - q_{\text{loss}})/[A_s(T_w - T_b)] \tag{15}$$

and the streamwise heat conduction loss along the channel walls. The power generated from the heaters is calculated from the heater resistance and the voltage.

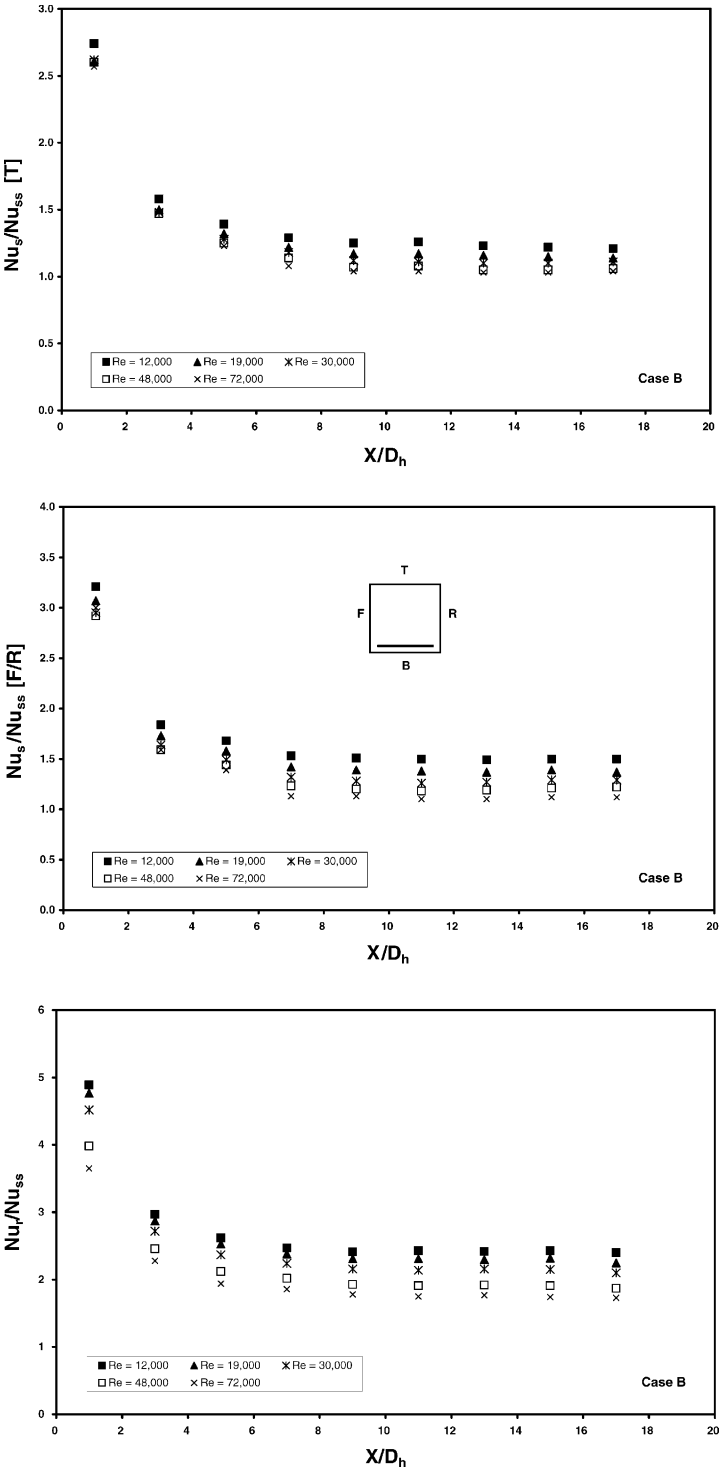

Fig. 5. Axial heat transfer distributions for one-ribbed wall channel.

The distribution of the bulk temperature is evaluated from energy balance in conjunction with the sum of the net rates of heat transfer from the four channel walls to the air, the air mass flow rate, and the inlet air bulk temperature.

The local (regionally averaged) Nusselt number is normalized by the Nusselt number for fully developed turbulent flow in a smooth circular tube correlated by McAdams/Dittus-Boelter as:

$$Nu_r/Nu_{ss} = (h_r D_h/k)/(0.023Re^{0.8}Pr^{0.4}) \quad \text{or} \quad Nu_s/Nu_{ss} = (h_s D_h/k)/(0.023Re^{0.8}Pr^{0.4}) \tag{16}$$

The maximum uncertainty in the heat transfer coefficient and friction factor is estimated to be less than 7% and 8%, respectively, by using the uncertainty estimation method of Kline and McClintock [20].

4. Results and discussion

4.1. Regionally averaged heat transfer

The regionally averaged heat transfer results are computed and plotted as normalized Nusselt number

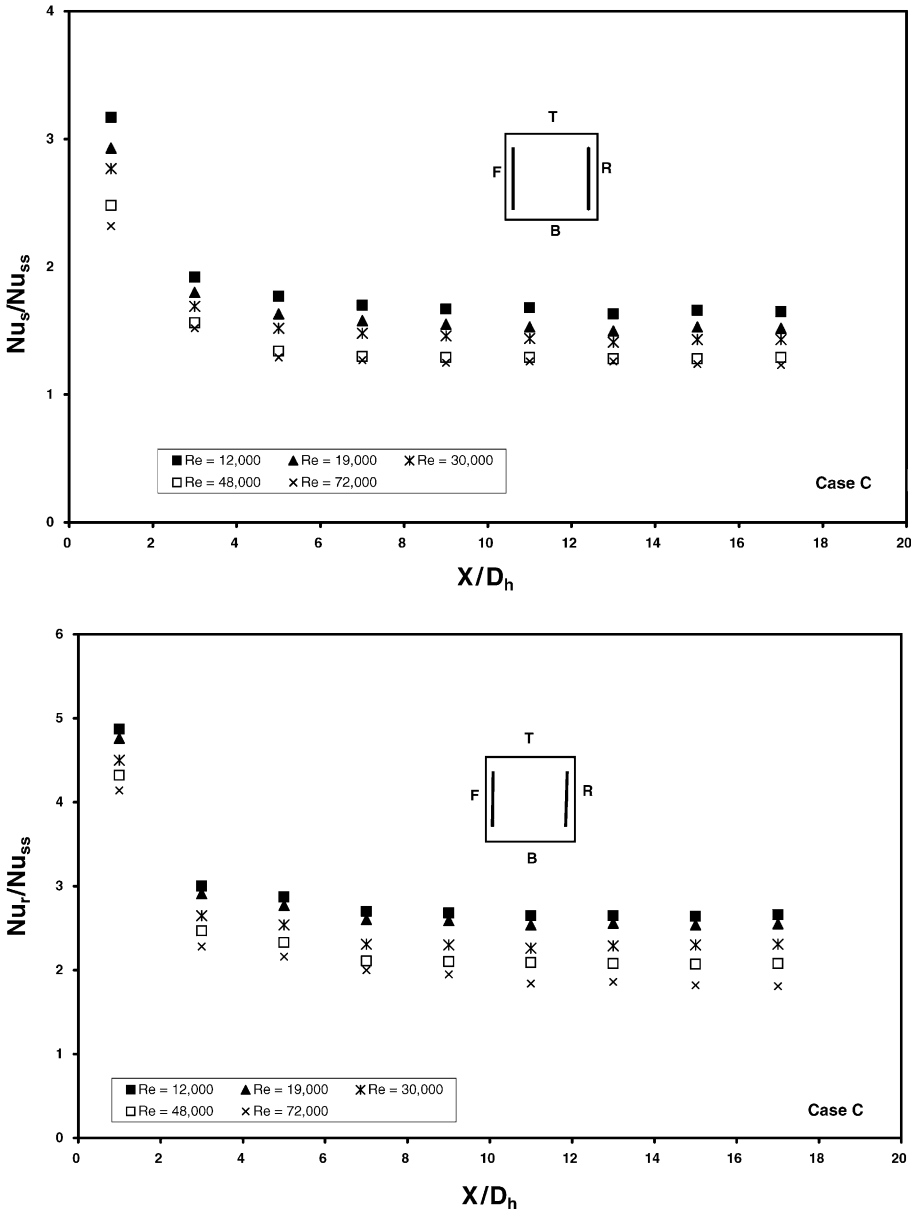

Fig. 6. Axial heat transfer distributions for two-ribbed wall channel.

ratio versus normalized axial distance from the channel entrance. Fig. 4 represents the regionally averaged Nusselt number distributions for the smooth case. The Nusselt number ratio decreases with increasing axial distance and reaching a constant value in the fully developed region for a given Reynolds number. The results

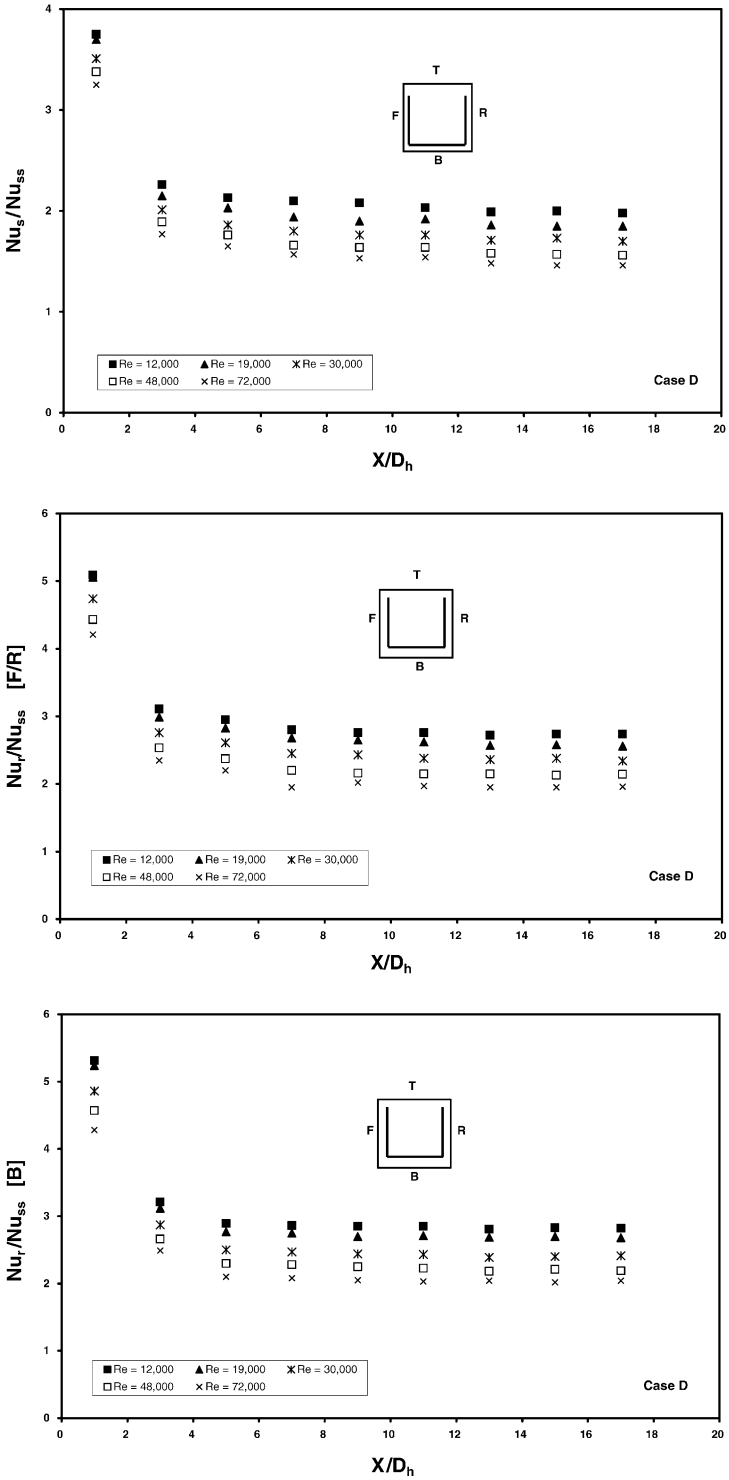

Fig. 7. Axial heat transfer distributions for three-ribbed wall channel.

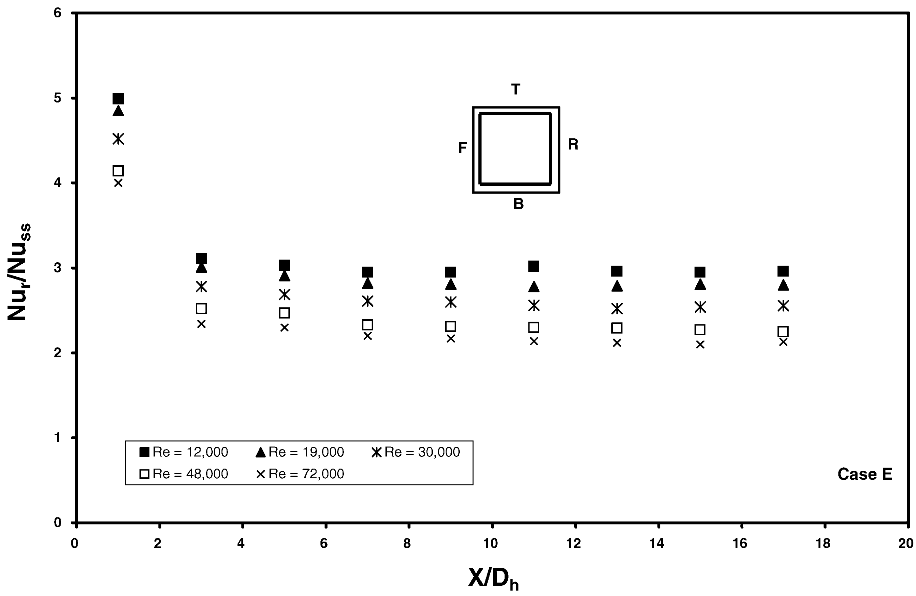

Fig. 8. Axial heat transfer distributions for three-ribbed wall channel.

are as expected and compares well with the McAdams/Dittus-Boelter correlation. Figs. 5–8 show the results for the cases with one, two, three, and four-ribbed channel walls. These figures show the regionally averaged ribbed-side and smooth-side Nusselt number ratio distributions for full transverse ribs versus normalized axial distance. The results show that for all the cases, the local Nusselt number ratio on ribbed as well as on smooth walls decreases with increasing Reynolds number. The Nusselt number ratio reaches almost a constant value in the fully developed region.

4.2. Channel averaged heat-transfer and pressure drop

Fig. 9 shows the average Nusselt number ratio, Nu/Nu_{ss}, versus Reynolds number for cases A to E. The ribbed-side and smooth-side Nusselt number ratios are the average values of the regional ribbed wall and smooth wall Nusselt number ratios for the fully developed heated channel length ($X/D_h = 6.0$–18.0) respectively. It is evident from the results that the channel average Nusselt number ratio decreases as Reynolds number increases.

Case B with one ribbed wall shows a heat transfer enhancement of 2.43–1.78 times over the range of Reynolds numbers from 12,000 to 75,000. The Nusselt number ratios on the adjacent and opposite smooth sides are in the range of 1.51–1.14 (about 40% decrease from that of the ribbed side) and 1.24–1.04 (about 48% decrease from that of the ribbed side) respectively. The channel with two opposite ribbed walls, Case C, exhibits enhancement of 2.64–1.92 on ribbed walls and of 1.67–1.26 on smooth walls.

This constitutes to an increase of ribbed wall heat transfer of about 6% over Case B. Case D with ribs on three walls gives an increase of ribbed wall heat transfer of about 5% (2.81–2.01) over case with ribs on two walls. The ribbed wall in between the other two ribbed walls shows slightly higher values. On the smooth wall, the Nusselt number ratios are about 22% higher (2.02–1.50) than the corresponding values of Case C. The fully ribbed channel, Case E, exhibits the highest heat transfer performance which is about 7% increase (2.99–2.12) over the ribbed walls values of Case D. This trend of heat transfer enhancement with the increase in the number of ribbed walls is due to the increase in the level of turbulence generated in the channel.

Fig. 10 compares the friction factor ratio for all the cases studied. The calculation of the friction factor takes into account the temperature variation in the channel. The results show that the friction factor ratio increases with increasing Reynolds number. Ribs on all four walls of the channel, Case E, create maximum pressure-drop/friction-factor that is about 9.50 times f_{ss} for a Reynolds number of 30,000. The flow encounters greater resistance with each additional ribbed wall and thus experiences higher friction. The friction factor ratio, f_r/f_{ss}, for the smooth channel is slightly higher when compared to the calculated Blasius values for a smooth circular pipe. For comparison at Reynolds number of 30,000, the friction ratio is 3.14, 5.39, 7.30, and 9.50 for cases B, C, D and E, respectively. This reflects a 214% increase of

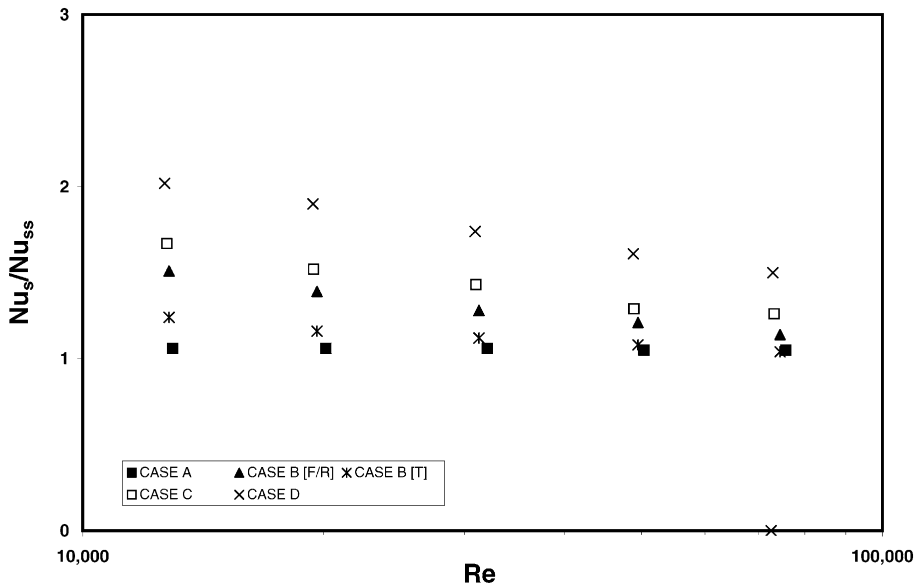

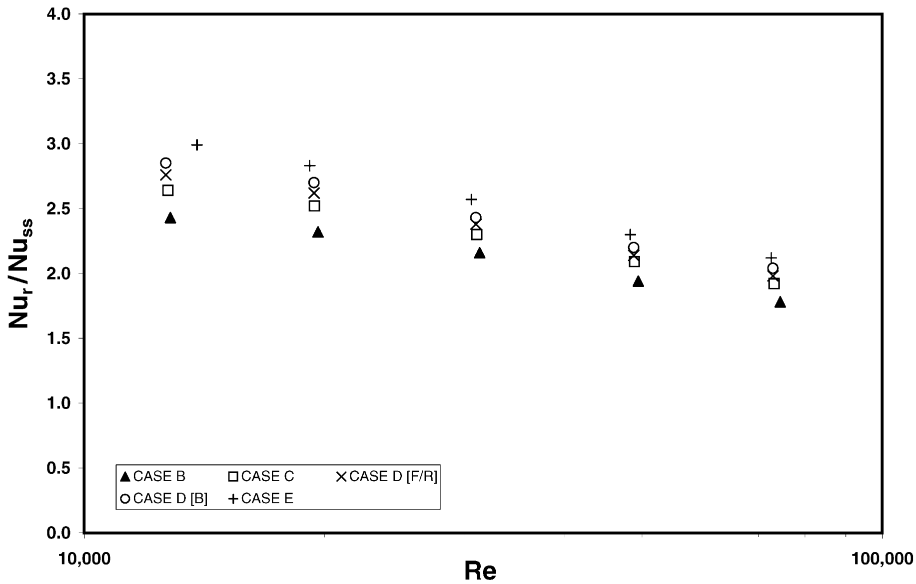

Fig. 9. Average Nusselt number ratio versus Reynolds number.

Case B compared to Case A, a 72% increase of Case C compared to Case B, a 35% increase of Case D compared to Case C, and a 30% increase of Case E compared to Case D.

4.3. Heat transfer performance

Fig. 11 represents the Nusselt number ratio (ribbed-side and smooth-side) versus the friction factor ratio for the cases B to E. The results show that the Nusselt number ratio decreases while the friction factor ratio increases with increasing Reynolds numbers as discussed in Section 4.2. This means that the heat transfer performance decreases with increasing Reynolds numbers. The Case C with full transverse ribs on two opposite walls provides 2.64–1.92 times ribbed side heat transfer (Nu_r) enhancement and 4.35–6.29 times pressure drop penalty with increasing Reynolds number. On the other hand, Case E with four ribbed walls enhances the ribbed side heat transfer by 2.99–2.12 times but also increases the pressure drop by respectively 7.96–11.45 times with increasing Reynolds number. Fig. 12 represents a com-

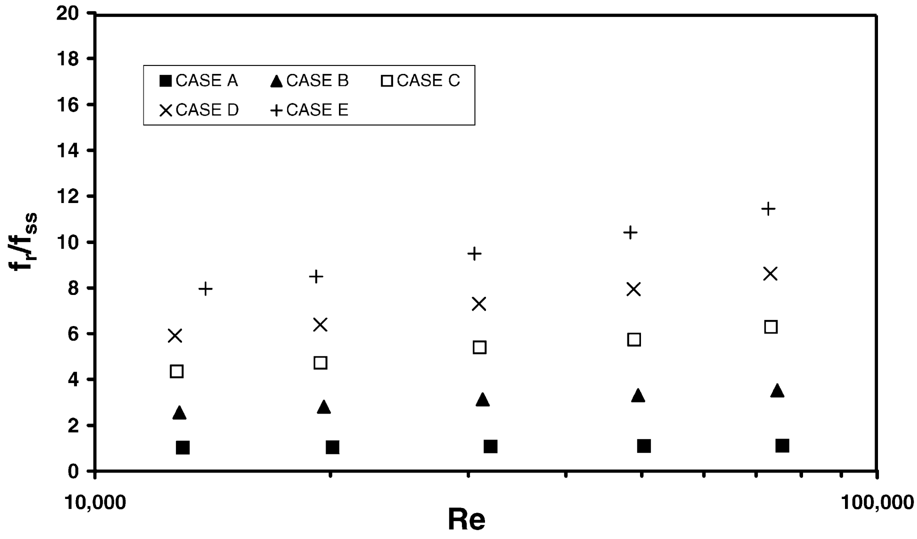

Fig. 10. Average friction factor ratio versus Reynods number.

parison of performance of the cases studied over the range of Reynolds numbers. One of the performance evaluation criteria is to compare the increased heat transfer for the same surface area and pumping power, $[\{St_r/St_{ss}\}/\{f_r/f_{ss}\}^{1/3}]$. The results show that the variation in the values of this performance factor is 1.78–1.17, 1.62–1.04, 1.55–1.00, and 1.50–0.95 for cases B, C, D, and E, respectively. The performance decreases with each additional ribbed wall by 11%, 5%, and 2.5% at a typical Reynolds number of 30,000.

4.4. Friction and heat transfer correlations

As discussed earlier, the wall similarity laws were employed to correlate the friction and heat transfer data for fully developed turbulent flow in a square channel with one, two, three, and four ribbed walls. According to the friction similarity law, the measured friction factor, f_r, the ribbed and smooth wall cross-sectional widths, C_r and C_s, channel width and height, W and H, the rib height-to-hydraulic diameter ratio, e/D_h, and the Reynolds number are correlated with friction roughness function, $R(e^+)$, as given in Eq. (6). The plot of $R(e^+)$ versus the roughness Reynolds number, (e^+) is shown in Fig. 13. The friction roughness function correlation of the present investigation is given by Eq. (17) and the deviation is within 4%. Note that experimental data for rectangular channels (AR = 0.5) with varying number of ribbed walls, Chandra et al. [18] are also included in the correlation for comparison.

$$R(e^+) = 3.44 \quad \text{for } e^+ \geqslant 120 \tag{17}$$

It is evident that the friction roughness function is independent of the roughness Reynolds number for all the cases studied. This implies that the four-sided rib channel friction factor is almost independent of Reynolds number. The correlated value of the function $R(e^+)$ of the present study for $P/e = 8$ is 7.5% higher than the correlated value of Han [3] for $P/e = 10$.

The measured ribbed side Stanton number, St_r, the calculated four-sided rib wall friction factor, f_{rr}, the ribbed and smooth wall cross-sectional widths, C_r and C_s, and the Reynolds number are correlated with the heat transfer roughness function, $G(e^+)$, as given in Eq. (10). A plot of $G(e^+)$ versus the roughness Reynolds number, (e^+), is shown in Fig. 14. The heat transfer roughness function, $G(e^+)$, increases with increasing roughness Reynolds number, (e^+), for all the rib configurations. The heat transfer roughness function correlation of the present investigation is given by Eq. (18) and the deviation of the equation is within 10%. Note that experimental data for rectangular channels (AR = 0.5) with varying number of ribbed walls, Chandra et al. [18] are also included in the correlation for comparison.

$$G(e^+) = (e^+)^{0.47} \quad \text{for } e^+ \geqslant 120 \tag{18}$$

The results are comparable with Han [3]. In the present study, actual St_{rr} data is used rather than assuming St_{rr} equals St_r. For all rib configurations (number of ribbed walls in a channel) and flow Reynolds number, the heat transfer coefficient can be predicted from the experimental values of heat transfer roughness function, $G(e^+)$, for a given roughness Reynolds number, (e^+).

With the $R(e^+)$ and $G(e^+)$ correlations, the rib channel friction factor (f_r) and heat transfer coefficient (St_r) can be predicted for a rectangular channel for a given aspect ratio (AR), Re, e/D_h, and the number of ribbed sides.

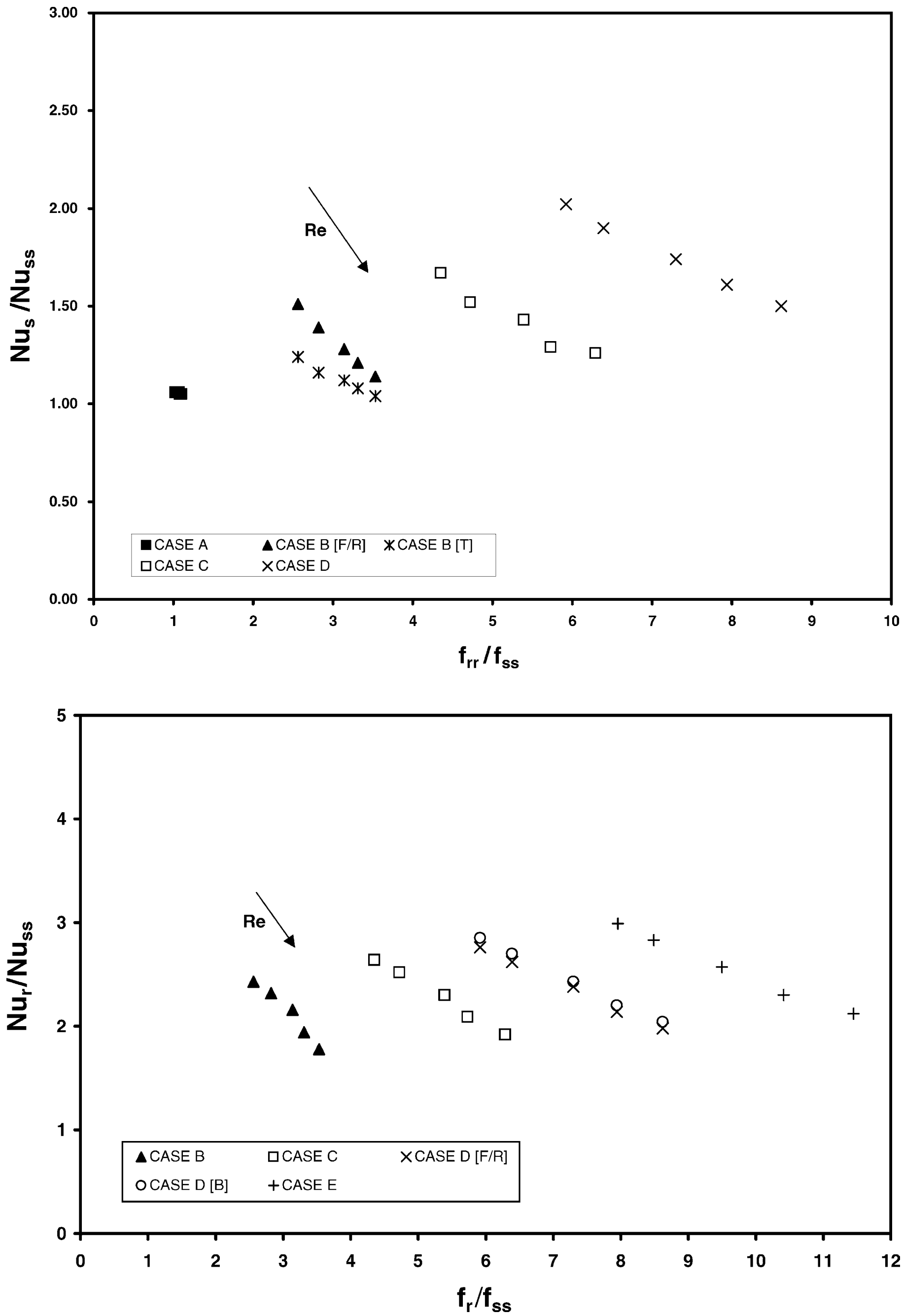

Fig. 11. Average Nusselt number ratio versus friction factor ratio.

To predict the average friction factor, f_r: $R(e^+)$ is obtained from the correlation, Eq. (17). Then the four-sided ribbed channel friction factor f_{rr} is calculated with Eq. (6). Finally, the friction factor, f_r, is calculated using Eq. (9).

To predict the heat transfer coefficient, St_r: the Roughness Reynolds number (e^+) is calculated using Eq. (7). Then the $G(e^+)$ is obtained from the correlation, Eq. (18). The ribbed wall on all four sides Stanton number, St_{rr}, is calculated with Eq. (10). Finally, the ribbed wall Stanton number, St_r, is calculated from Eq. (11).

One of the purposes of the present investigation is to confirm the validity of the method used in the past [1,3]

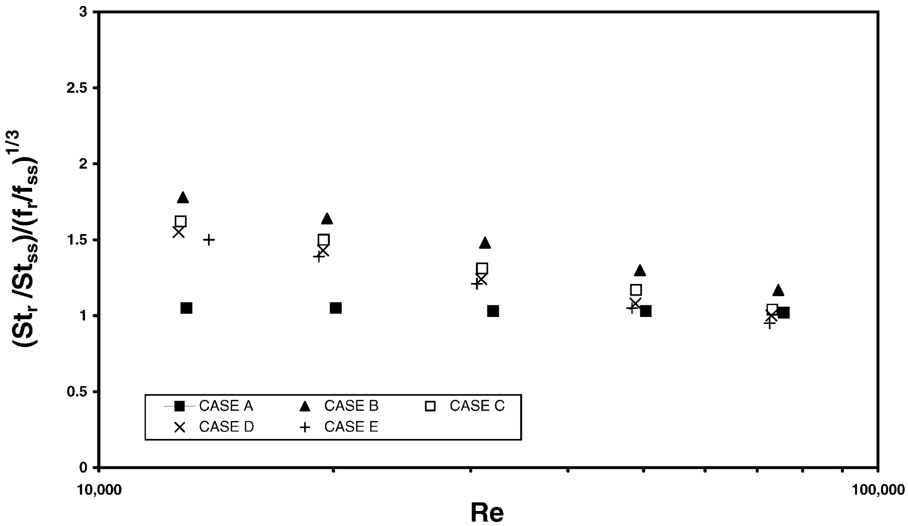

Fig. 12. Enhanced heat transfer for a constant pumping power.

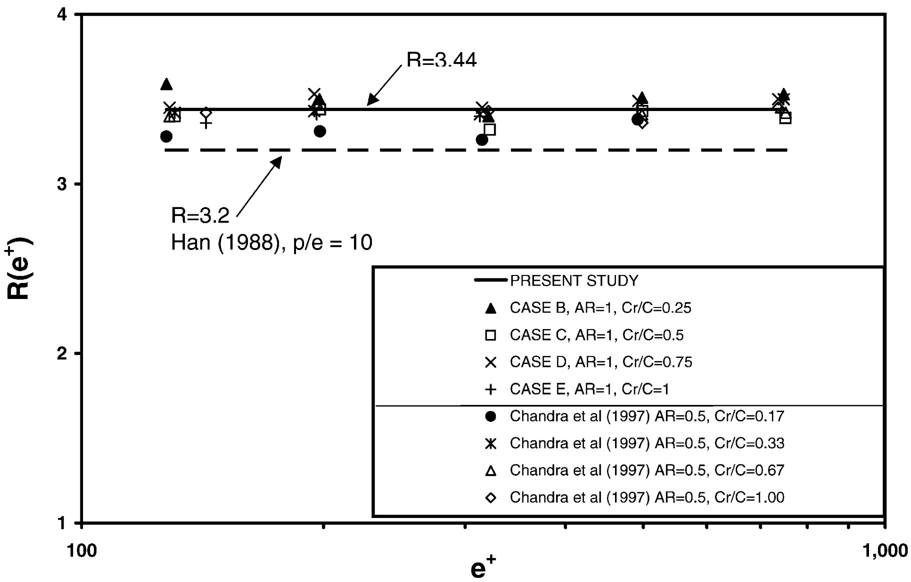

Fig. 13. Ribbed channel friction correlation.

to predict the friction factor for four-sided ribbed wall channel. The experiments conducted in the past were with channels with two opposite rib-roughened walls. The friction factor for four-sided ribbed duct is needed to correlate the friction roughness and heat transfer roughness functions. As explained earlier, in the present study, the four-sided friction factor, f_{rr}, is calculated by Eq. (9) for channels with one, two, and three ribbed walls. These values are then compared with the experimental values of Case E with four ribbed walls. Fig. 15 shows these results as a plot of f_{rr}/f_{ss} versus Reynolds number. It is evident that the present predictions of four-sided ribbed channel friction factor values used Eq. (9) for cases with fewer ribbed walls agree with the experimental results. This further confirms the validity of the previous correlations by Han [1,3] using rectangular channel data with only two opposite ribbed walls.

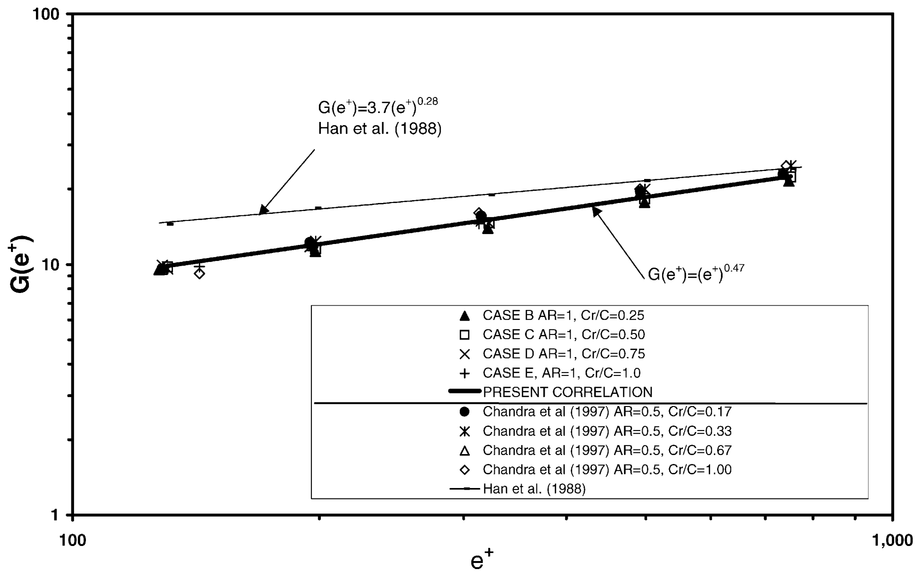

Fig. 14. Ribbed channel heat transfer correlation.

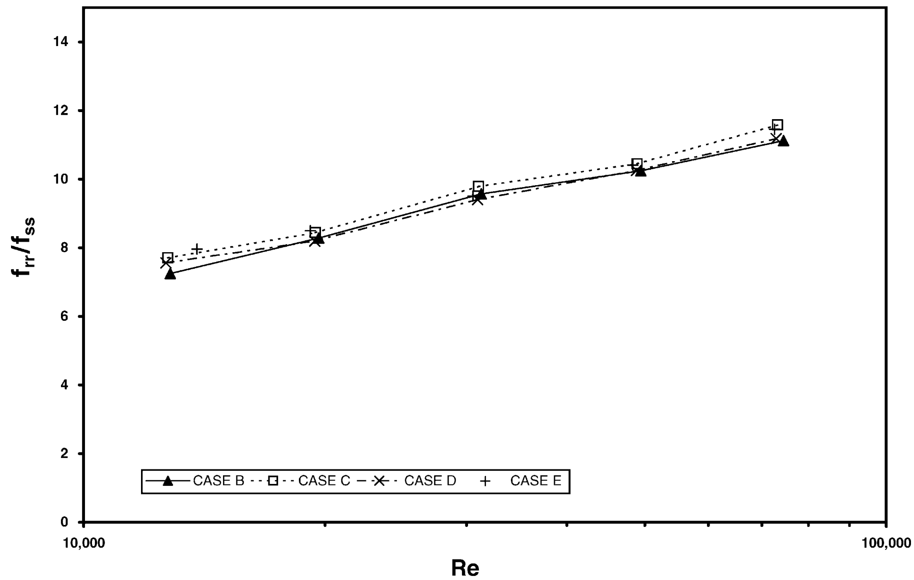

Fig. 15. Validity of the prediction equation for the friction factor of four-ribbed.

5. Conclusions

1. The regionally averaged Nusselt number ratio decreases with increasing Reynolds number for the range of the test data. The Nusselt number ratio reaches almost a constant value in the fully developed region, $X/D_h > 6.0$.
2. The heat transfer is enhanced with the increase in the number of ribbed channel walls from 2.16 for one ribbed walls case to 2.57 for four ribbed walls case ($Re = 30,000$).
3. The channel with two opposite ribbed walls show a 6% increase in heat transfer over the one ribbed walls case. The three ribbed walls case shows a 5% increase over two ribbed walls case. The four ribbed walls case shows an increase of 7% over the three ribbed walls case.
4. Friction factor ratio increases with increasing Reynolds number. For $Re = 30,000$, experiments reveal

a 214% increase of Case B compared to Case A, a 72% increase of Case C compared to Case B, a 35% increase of Case D compared to Case C, and a 30% increase of Case E compared to Case D.
5. Heat transfer performance decreases with increasing Reynolds number and with each additional ribbed wall.
6. The friction roughness function, $R(e^+)$, is independent of the roughness Reynolds number for all the cases studied for $P/e = 8$, and is equal to 3.44 which is 7.5% higher than Han [3] for $P/e = 10$.
7. The heat transfer roughness function, $G(e^+)$, increases with increasing roughness Reynolds number. The correlation of the function compares well with Han [3]. In the present study, actual St_{rr} data is used rather than assuming St_{rr} equals St_r.
8. Friction factor and heat transfer coefficient (St) can be predicted for a rectangular channel for a given aspect ratio (AR), Re, e/D_h, and the number of ribbed sides from the friction roughness function, $R(e^+)$ and heat transfer roughness function, $G(e^+)$.
9. The past and the present predictions of four-sided ribbed channel friction factor values used for cases with fewer ribbed walls agree with the experimental results. The prediction method and the experimental data may be applied to the design of equipment, which require internal cooling passages with one, two, three, or four ribbed walls.

Acknowledgements

This work was sponsored by the National Science Foundation under Grant CTS 9116489. Their support is gratefully acknowledged.

References

[1] J.C. Han, Heat transfer and friction in channels with two opposite rib-roughened walls, J. Heat Transfer 106 (1984) 774–781.
[2] J.C. Han, J.S. Park, C.K. Lei, Heat transfer enhancement in channels with turbulence promoters, J. Eng. Gas Turbines Powers 107 (1985) 629–635.
[3] J.C. Han, Heat transfer and friction characteristics in rectangular channels with rib turbulators, J. Heat Transfer 110 (1988) 321–328.
[4] J.C. Han, J.S. Park, Developing heat transfer in rectangular channels with rib turbulators, Int. J. Heat Mass Transfer 31 (1988) 183–195.
[5] J.C. Han, S. Ou, J.S. Park, C.K. Lei, Augmented heat transfer in rectangular channels of narrow aspect ratios with rib turbulators, Int. J. Heat Mass Transfer 32 (1989) 1619–1630.
[6] J.C. Han, P.R. Chandra, S.C. Lau, Local heat/mass transfer distributions around sharp 180° turns in two-pass smooth and rib-roughened channels, Int. J. Heat Mass Transfer 110 (1988) 91–98.
[7] P.R. Chandra, J.C. Han, S.C. Lau, Effect of rib angle on local heat/mass transfer distribution in a two-pass rib-roughened channel, J. Turbomachinery 110 (1988) 233–241.
[8] P.R. Chandra, J.C. Han, Pressure drop and mass transfer in two-pass ribbed channels, J. Thermophys. Heat Transfer 3 (1989) 315–320.
[9] J.C. Han, P. Zhang, Pressure loss distribution in three-pass rectangular channels with rib turbulators, J. Turbomachinery 111 (1989) 515–521.
[10] J.C. Han, P. Zhang, Effect of rib-angle orientation on local mass transfer distribution in a three-pass rib-roughened channel, J. Turbomachinery 113 (1991) 123–130.
[11] S.C. Lau, R.D. McMillin, J.C. Han, Turbulent heat transfer and friction in a square channel with discrete rib turbulators, J. Turbomachinery 113 (1991) 360–366.
[12] S.C. Lau, R.D. McMillin, J.C. Han, Heat transfer characteristics of turbulent flow in a square channel with angled discrete ribs, J. Turbomachinery 113 (1991) 367–374.
[13] R.T. Kukreja, S.C. Lau, R.D. McMillin, P.R. Chandra, Effects of length and configuration of transverse discrete ribs on heat transfer and friction for turbulent flow in a square channel, ASME/JSME Thermal Engineering Joint Conference 3 213–218, Reno, Nevada, 1991.
[14] J. Nikuradse, Laws for flow in rough pipes, NACA TM 1292, 1950.
[15] D.F. Dipprey, R.H. Sabersky, Heat and momentum transfer in smooth and rough tubes in various Prandtl number, Int. J. Heat Mass Transfer 6 (1963) 329–353.
[16] R.L. Webb, E.R.G. Eckert, R.J. Goldstein, Heat transfer and friction in tubes with repeated-rib roughness, Int. J. Heat Mass Transfer 14 (1971) 601–617.
[17] J.C. Han, L.R. Glicksman, W.M. Rohsenow, An investigation of heat transfer and friction for rib-roughened surfaces, Int. J. Heat Mass Transfer 21 (1978) 1143–1156.
[18] P.R. Chandra, M.E. Niland, J.C. Han, Heat and friction analysis of turbulent flow in a rectangular channel with varying number of ribbed walls, J. Turbomachinery 119 (1997) 374–380.
[19] W.M. Kays, M.E. Crawford, Convective Heat and Mass Transfer, second ed, McGraw-Hill, New York, 1989.
[20] S.J. Kline, F.A. McClintock, Describing uncertainties in single sample experiments, Mech. Eng. 75 (1953) 3–8.